6-15-1979

Relations between amplitude reflectances and phase shifts of the p and s polarizations when electromagnetic radiation strikes interfaces between transparent media

R. M.A. Azzam
University of New Orleans, razzam@uno.edu

Recommended Citation

R. M. A. Azzam, "Relations between amplitude reflectances and phase shifts of the p and s polarizations when electromagnetic radiation strikes interfaces between transparent media," Appl. Opt. 18, 1884-1886 (1979)

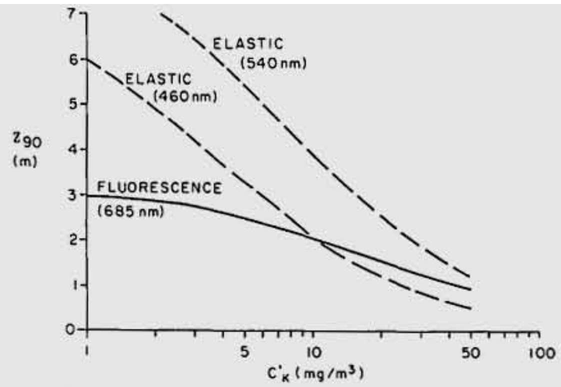

Fig. 1. The remote sensing penetration depth Z_{90} for *in vivo* fluorescence of chlorophyll *a* as a function of C'_K. Shown for comparison are the penetration depths associated with elastic scattering processes at 460 nm and 540 nm (*dashed curves*).

Note that ζ and hence Z_{90} depends on $E_d(\lambda)$, $a_c(\lambda)$, $K(\lambda)$, and μ'_0 but is independent of δ_0 and hence is independent of the quantum efficiency η. Also, the dependence of Z_{90} on the precise wavelength of the fluorescence λ_F is completely contained in the $K(\lambda_F)$ term.

Figure 1 gives this fluorescence penetration of C'_K along with the penetration depth for elastic processes $K(\lambda)^{-1}$ at 460 nm and 540 nm. The maximum penetration depth for fluorescent sensing is about 3 m and, because of the $K(\lambda)$ term in Eq. (5), varies significantly more slowly with pigment concentration than the penetration depths for elastic processes.

The computations presented here have been derived under the approximation that all the irradiance incident on the sea surface is in the form of direct sunlight. Although skylight makes a significant contribution to $E_d(\lambda)$ in the blue (i.e., 30–40% near 400 nm at high sun angles), it is believed that this will not seriously degrade the results presented in Fig. 1 for two reasons: first, a large fraction of the skylight will result from small angle aerosol scattering and hence arrive at the sea surface at nearly the same angle as the solar beam; and second, in the exact solution of the analogous problem for elastic scattering it was found[1] that the quasi-single-scattering prediction of the penetration depth (K^{-1}) was valid even in the case when the incident irradiance was totally diffuse.

This work received support from the National Aeronautics and Space Administration under contract NAS 5-22963. Portions of the work were completed while the author was on leave at the National Oceanic and Atmospheric Administration's Pacific Marine Environmental Laboratory in Seattle, Washington.

References

1. H. R. Gordon and W. R. McCluney, Appl. Opt. 14, 413 (1975).
2. H. R. Gordon, Appl. Opt. 17, 1893 (1978).
3. R. A. Neville and J. F. R. Gower, J. Geophys. Res. 82, 3487 (1977).
4. J. F. R. Gower and R. A. Neville, "A Method for the Remote Measurement of the Vertical Distribution of Phytoplankton in Sea Water," in *Procedures, Fourth Canadian Symposium on Remote Sensing*, Quebec City, May 1977 (Canadian Aeronautics and Space Administration, Ottawa, 1977).
5. H. R. Gordon, Appl. Opt. 18, 1161 (1979). This paper contains several typographical errors. These are: (1) Ω' should be μ' in Eq. 7, (2) Ω_E should be λ_E in Eq. 8, (3) the last line of Eq. 9 should read: $\times \exp[-K(\lambda_E)Z]\, f(\lambda_E,\lambda_F)d\lambda_E$, (4) the first sign in the equation defining $f(\lambda_E,\lambda_F)$ should be minus not plus, (5) the a_c scale in Fig. 3 is $\times 10^3$ not $\times 10^2$, and (6) in line 6 on page 1165 W m^{-1}/cm^2 should be mWm^{-1}/cm^2.
6. H. R. Gordon, O. B. Brown, and M. M. Jacobs, Appl. Opt. 14, 417 (1975).
7. R. I. Currie, Nature 193, 956 (1962).
8. J. Patterson and T. R. Parsons, Limnol. Oceanogr. 8, 335 (1963).
9. C. J. Lorenzen, Limnol. Oceanogr. 10, 482 (1965).
10. C. J. Lorenzen, Deep Sea Res. 13, 223 (1966).
11. R. C. Smith and K. S. Baker, Limnol. Oceanogr. 23, 247 (1978).
12. R. C. Smith and K. S. Baker, Limnol. Oceanogr. 23, 260 (1978).
13. This is defined to be the depth over which the number of downwelling quanta falls to $1/e$ of the number at the surface.
14. A. Morel and L. Prieur, Limnol. Oceanogr. 22, 709 (1977).
15. K. Ya Kondratev, *Radiation Characteristics of the Atmosphere and Earth's Surface* (Amerind Publishing Company, New Delhi, 1973).

Relations between amplitude reflectances and phase shifts of the *p* and *s* polarizations when electromagnetic radiation strikes interfaces between transparent media

R. M. A. Azzam

University of Nebraska Medical Center, Hematology Division and Department of Internal Medicine, Omaha, Nebraska 68105.

Received 18 December 1978.
0003-6935/79/121884-03$00.50/0.

When an electromagnetic plane wave strikes the planar interface between two linear homogeneous and isotropic media, the complex amplitude Fresnel reflection coefficients r_p and r_s for the parallel p (or TM) and perpendicular s (or TE) polarizations are interrelated by

$$r_p = r_s(r_s - \cos 2\phi)/(1 - r_s \cos 2\phi), \tag{1}$$

where ϕ is the angle of incidence.[1] We assume the $\exp(j\omega t)$ time dependence and p and s directions according to the Nebraska (Muller) conventions.[2]

If the medium of incidence is transparent and the medium of refraction is absorbing, both r_p and r_s are in general complex, and the function $r_p = f(r_s)$ of Eq. (1) can be studied graphically as a conformal mapping between the complex planes of r_s and r_p.[1] In this Letter we examine the special but important case when both media are transparent.

In the absence of absorption two situations are physically distinguishable:

(1) Partial (internal or external) reflection, in which case r_s and r_p are real and $|r_\nu| < 1$, $\nu = p,s$. Here we plot r_p vs r_s as real variables with the angle of incidence ϕ as a parameter using Eq. (1).

(2) Total (internal) reflection, in which case $|r_\nu| = 1$, $\nu = p,s$. If we substitute $r_\nu = \exp(j\delta_\nu)$ in Eq. (1) we get

Equation (2) is equivalent to a single real relation between δ_p and δ_s, namely,

$$\delta_p = \delta_s + \arctan\left(\frac{\sin\delta_s}{\cos\delta_s - \cos 2\phi}\right) + \arctan\left(\frac{\sin\delta_s \cos 2\phi}{1 - \cos\delta_s \cos 2\phi}\right), \tag{3}$$

as may be obtained by taking the argument of both sides of Eq. (2). Equation (3) provides a direct relation between the phase shifts δ_p and δ_s that the p- and s-polarized components of the incident wave experience upon total (internal) reflection.[3] Here we also plot δ_p vs δ_s with the angle of incidence ϕ as a parameter.

Figure 1 shows r_p vs r_s (denoted by RP and RS) at one angle

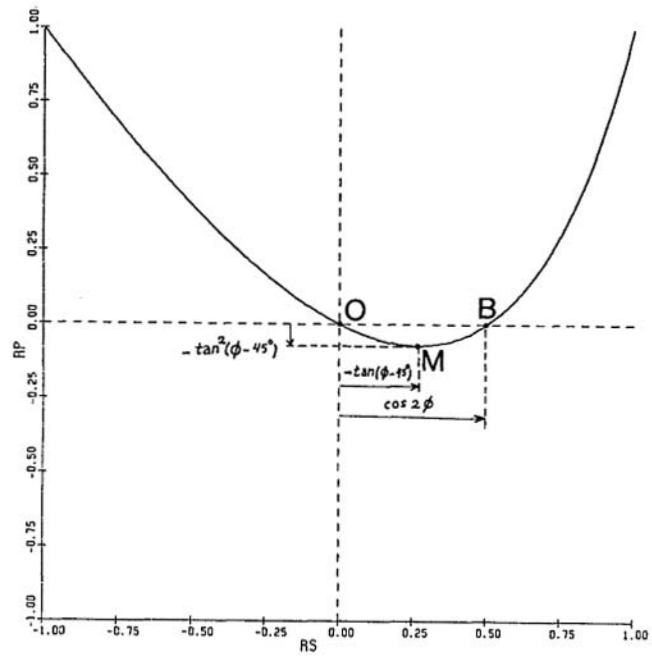

Fig. 1. Relation between Fresnel's reflection coefficients for the p and s polarizations (denoted by RP and RS) at a fixed angle of incidence ϕ (taken here equal to 30°). The curve represents partial reflection at interfaces between transparent media. The significance of the points marked on the curve is discussed in the text.

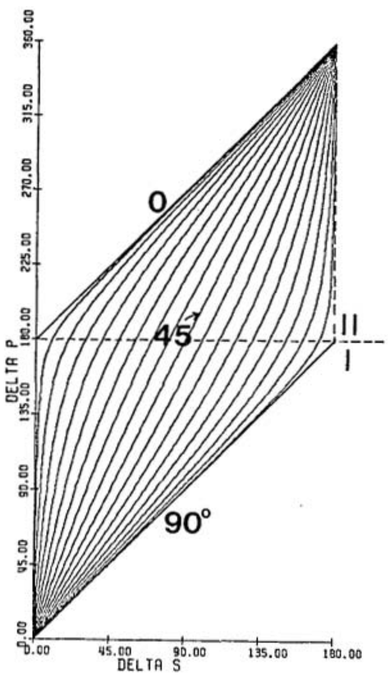

Fig. 3. Relation between the total-reflection phase shifts δ_p and δ_s for the p and s polarizations (denoted by DELTA P and DELTA S) at 19 angles of incidence between 0° and 90° in equal steps of 5°. This figure applies to all possible instances of total reflection[9] and throughout the electromagnetic spectrum.

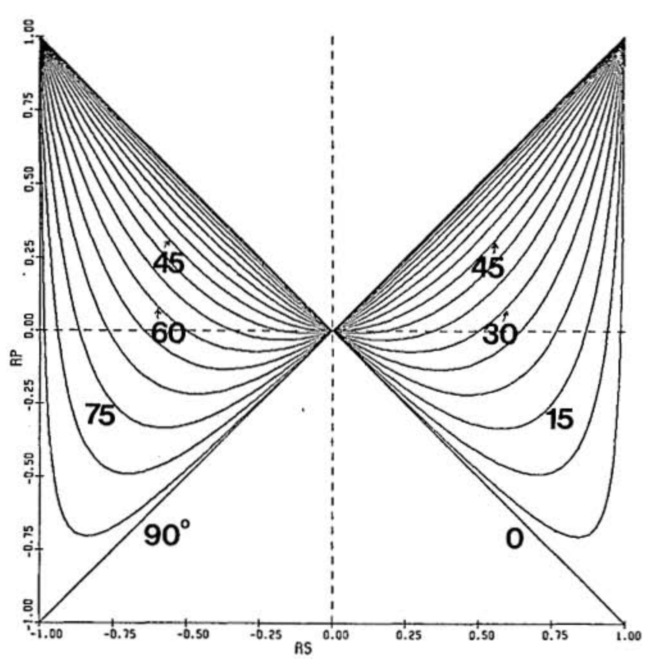

Fig. 2. Relation between Fresnel's reflection coefficients for the p and s polarizations (denoted by RP and RS) at 19 angles of incidence between 0° and 90° in equal steps of 5°. This figure applies to partial (internal and external) reflection at all possible interfaces between transparent media and throughout the electromagnetic spectrum.

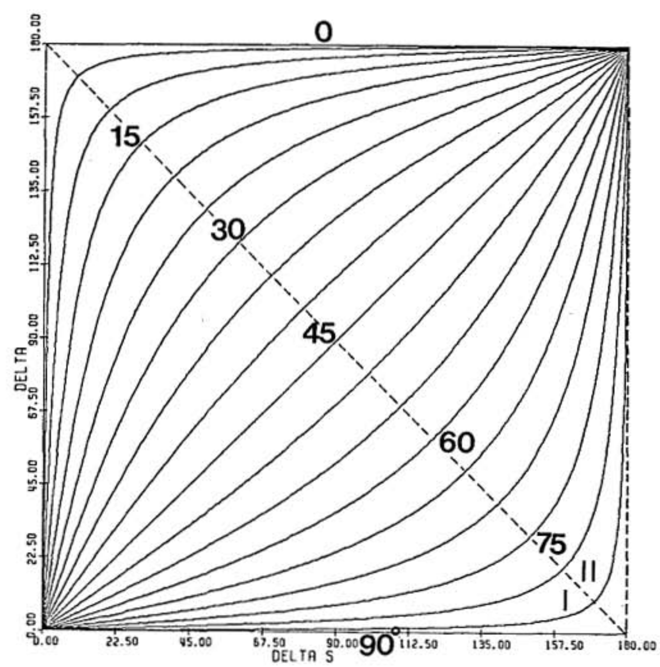

Fig. 4. Relation between the total-reflection phase shifts $\Delta = \delta_p - \delta_s$ and δ_s (denoted by DELTA and DELTA S) at 19 angles of incidence between 0° and 90° in equal steps of 5°. This figure applies to all possible instances of total reflection[10] and throughout the electromagnetic spectrum.

of incidence ϕ (30°). The origin $O(r_s = r_p = 0)$ represents the limiting case of wave reflection from a vanishing interface when the two surrounding media become the same. The point $B(r_s = \cos 2\phi,\ r_p = 0)$ represents reflection at the Brewster angle. The point of minimum $r_p M[r_s = -\tan(\phi - 45°),\ r_p = -\tan^2(\phi - 45°)]$ corresponds to wave refraction at 45°.[4] From Fig. 1 notice that while there is only one value of r_p for each value of r_s, a given value of r_p leads to two values of r_s. (An r_p = constant straight line intersects the curve of r_p vs r_s at two points, or does not intersect it at all. At M the two points of intersection coincide.) From Eq. (1) the two values of r_s that correspond to the same value r_p are given by $r_s = 0.5 \cos 2\phi(1 - r_p) \pm [r_p + 0.25 \cos^2 2\phi(1 - r_p)^2]^{1/2}$.

Figure 2 shows a collective view of r_p vs r_s at 19 equispaced angles of incidence from 0° to 90° in steps of 5°. The following features can be deduced from Fig. 2:

(1) If we exclude normal and grazing incidence ($\phi = 0, 90°$), as r_s scans the full range from −1 to +1, r_p scans (twice) the truncated interval, $-\tan^2(\phi - 45°) \le r_p \le 1$, at any given angle of incidence[5] ϕ.

(2) The limiting cases of normal incidence, $\phi = 0$, and grazing incidence, $\phi = 90°$, are represented by the straight lines $r_p = -r_s$ and $r_p = r_s$, respectively. These lines define the boundaries of the domain of all physically possible pairs (r_s, r_p), where $|r_p| \le |r_s|$.

(3) The curve of r_p vs r_s becomes the symmetrical parabola $r_p = r_s^2$ when the angle of incidence is 45°.[6–8]

(4) Two curves of r_p vs r_s associated with two angles of incidence equally above and below 45° (i.e., $\phi = 45° \pm \theta$) are mirror images of one another with respect to the $r_s = 0$ axis.

(5) The locus of the point of minimum r_p (M in Fig. 1), as the angle of incidence is varied, is the inverted parabola $r_p = -r_s^2$. This locus represents all possible instances of wave refraction at 45°.[4]

(6) When $r_s = -1$, we have $r_p = 1$ at all angles of incidence except grazing incidence, $0 \le \phi < 90°$; when $\phi = 90°$, $r_p = -1$. Likewise, when $r_s = 1$, we have $r_p = 1$ at all angles of incidence except normal incidence, $0 < \phi \le 90°$; when $\phi = 0$, $r_p = -1$.

Figure 3 gives δ_p vs δ_s (denoted by DELTA P and DELTA S) under conditions of total reflection[9] as computed using Eq. (3) for 19 angles of incidence from 0° to 90° in equal steps of 5°. The following can be noted from Fig. 3:

(1) The limiting cases of normal incidence, $\phi = 0$, and grazing incidence, $\phi = 90°$, are represented by the straight lines $\delta_p = \delta_s + 180°$ and $\delta_p = \delta_s$, respectively. These lines bound the domain of all permissible pairs (δ_s, δ_p), where $\delta_s \le \delta_p \le \delta_s + 180°$.

(2) Incidence at 45° is represented by the straight line[8] $\delta_p = 2\delta_s$.

(3) Two curves of δ_p vs δ_s for two angles of incidence equally above and below 45° (i.e., $\phi = 45° \pm \theta$) are symmetrical with respect to the straight line $\delta_p = 2\delta_s$, in the sense that any δ_p = constant straight line intersects the two curves at two points that are equidistant from the point of intersection of the same straight line with $\delta_p = 2\delta_s$.

For completeness, we show in Fig. 4 $\Delta = \delta_p - \delta_s$ (denoted by DELTA) vs δ_s (denoted by DELTA S) at the same angles of incidence as in Fig. 3. Both δ_s and Δ are limited between 0° and 180°.[10] Mirror reflection with respect to the straight line $\Delta = \delta_s$ ($\phi = 45°$) relates any two Δ vs δ_s curves at $\phi = 45° \pm \theta$. This symmetry property is somewhat simpler than that stated above for the δ_p vs δ_s curves.

Finally, we emphasize that all the results presented here are valid independent of the specific media that define the interface and are applicable throughout the electromagnetic spectrum.

The author is now with the Department of Electrical Engineering, School of Engineering, University of New Orleans, Lakefront, New Orleans, Louisiana 70122.

References

1. R. M. A. Azzam, J. Opt. Soc. Am. (in press).
2. R. H. Muller, Surf. Sci. **16**, 14 (1969).
3. Equation (3) can be obtained by deleting the relative refractive index n as the common variable between δ_s and δ_p expressed as functions of n. Such functions can be found, for example, in M. Born and E. Wolf, *Principles of Optics* (Pergamon, New York, 1975), p. 49.
4. R. M. A. Azzam, J. Opt. Soc. Am. **68**, 1613 (1978).
5. Values of r_p in the remaining interval, $-1 \le r_p < -\tan^2(\phi - 45°)$, make r_s complex. This interesting situation is possible only in the presence of absorption and is discussed in Ref. 1.
6. S. P. F. Humphreys-Owen, Proc. Phys. Soc. London **77**, 949 (1961).
7. D. W. Berreman, J. Opt. Soc. Am. **56**, 1784 (1966).
8. R. M. A. Azzam, Opt. Acta **26**, 113 (1979).
9. For total internal reflection at interfaces between transparent media at a given angle of incidence, the maximum attainable phase shift for the s polarization is equal to double the angle of incidence, $\delta_s = 2\phi$, and occurs when the ratio of refractive indices of the two media tends to infinity. The associated phase shift for the p polarization reaches a maximum of π. It follows that, in Fig. 3, δ_p and δ_s for total reflection at interfaces between transparent media are confined to the domain denoted by I below the horizontal straight line $\delta_p = 180°$, which is also the locus of $\delta_s = 2\phi$. Domain II, above this line, represents total reflection at an interface between a transparent medium and a medium with a negative real dielectric constant (e.g., a plasma). The phase shifts in this case are also interrelated by Eq. (3).
10. In Fig. 4, the diagonal straight line $\Delta = 180° - \delta_s$ (= $180° - 2\phi$) defines the boundary between two domains I and II with significance as indicated in the foregoing footnote.

Moiré strain analysis in cryogenic environments

R. E. Rowlands and P. O. Lemens

The authors are with University of Wisconsin, Department of Engineering Mechanics, Madison, Wisconsin 53706.
Received 18 December 1978.
0003-6935/79/121886-02$00.50/0.

Contemporary demands such as superconducting magnets for energy storage operating at cryogenic environments necessitate the development of adequate strain measuring techniques under such conditions. While commercially available electrical strain gauges are employed at cryogenic temperatures, they are less than adequate. Moreover, the full-field capability of optical methods such as moiré warrants their development in cryogenic environments. It is the purpose of this Letter to describe the extension of moiré analysis of a component contained in liquid nitrogen (77 K). Moiré is demonstrated both with and without a tenfold fringe multiplication. The authors are unaware of any previously published application of moiré under cryogenic conditions.

Moiré is extremely well suited for strain (stress) analysis and metrology of physical components at room and elevated temperatures and under extreme conditions of loading.[1,2] The method records the basis of continuum physics, i.e., dis-